View metadata, citation and similar papers at core.ac.uk

brought to you by CORE

provided by Missouri University of Science and Technology (Missouri S&T): Scholars' Mine

Missouri University of Science and Technology

Scholars' Mine

International Conference on Case Histories in Geotechnical Engineering

(2008) - Sixth International Conference on Case Histories in Geotechnical Engineering

16 Aug 2008, 8:45am - 12:30pm

Prediction of Post-Earthquake Failure for a Near-Shore Slope in a Low Seismic Region

Mahmood Seid-Karbasi
Golder Associates Ltd., Burnaby, B.C, Canada

James Ji
Golder Associates Ltd., Burnaby, B.C, Canada

Upul Atukorala
Golder Associates Ltd., Burnaby, B.C, Canada

Peter Byrne
University of British Columbia, Vancouver, B.C, Canada

Follow this and additional works at: https://scholarsmine.mst.edu/icchge

 Part of the Geotechnical Engineering Commons

Recommended Citation

Seid-Karbasi, Mahmood; Ji, James; Atukorala, Upul; and Byrne, Peter, "Prediction of Post-Earthquake Failure for a Near-Shore Slope in a Low Seismic Region" (2008). *International Conference on Case Histories in Geotechnical Engineering*. 19.
https://scholarsmine.mst.edu/icchge/6icchge/session03/19

This Article - Conference proceedings is brought to you for free and open access by Scholars' Mine. It has been accepted for inclusion in International Conference on Case Histories in Geotechnical Engineering by an authorized administrator of Scholars' Mine. This work is protected by U. S. Copyright Law. Unauthorized use including reproduction for redistribution requires the permission of the copyright holder. For more information, please contact scholarsmine@mst.edu.


6th International Conference on
Case Histories in Geotechnical Engineering, Arlington, VA, August 11-16, 2008

PREDICTION OF POST-EARTHQUAKE FAILURE FOR A NEAR-SHORE SLOPE IN A LOW SEISMIC REGION

Mahmood Seid-Karbasi,
Ph.D. Candidate
Golder Associates Ltd.
Burnaby, B.C, Canada

James Ji
Ph.D., P. Eng.
Golder Associates Ltd.
Burnaby, B.C, Canada

Upul Atukorala
Ph.D., P. Eng.
Golder Associates Ltd.
Burnaby, B.C, Canada

Peter Byrne
Ph.D., P. Eng.
University of British Columbia
Vancouver, B.C, Canada

ABSTRACT

Liquefaction of water-saturated sandy soils remains a major concern in geotechnical earthquake engineering. Experience from past earthquakes indicates that large lateral spreads and flow slides in sand deposits have taken place in coastal and river areas not only during shaking but also some time after earthquake shaking ceases. The ground slopes in these slides were often gentler than a few percent. Recent research including physical model tests and numerical investigations indicates that the presence of a low permeability silt or clay layer as a hydraulic barrier may be responsible for some of the historical and seemingly unexplainable landslides.

This paper describes the results of a coupled stress-flow analysis carried out for a near-shore LNG import terminal to be founded on a moderate submarine slope comprising a liquefiable sand layer overlain by a clay layer located in a region with moderate seismic risk (PGA< 0.15g). Artesian water conditions are present at the site due to the presence of the hydraulic barrier layer and the mountain slopes near the shoreline. An effective-stress based approach was employed to analyze the excess pore pressure generation in the sand layer associated with earthquake loading. The analyses showed that pore pressure redistribution during and after earthquake shaking may result in continued displacements after shaking has ceased, although the magnitude of displacements at the end of shaking was not very large.

INTRODUCTION

Earthquakes have caused severe damage to onshore and off-shore infrastructures such as buildings, bridges, ports or terminals, dams, lifelines, particularly where soil liquefaction was involved. Liquefaction of water saturated sandy soils is a major concern in geotechnical engineering in seismic areas. Liquefaction can occur in saturated granular soils when seismic excitations result in the generation of high pore water pressures and large reductions in soil shear stiffness and strength that lead to large ground deformations or failures. Although notable advancements have been made in understanding the mechanism of soil liquefaction and the remedial measures for dealing with the issue over the past 2 to 3 decades, most of the significant progress has been confined to assessing the likelihood of liquefaction triggering under undrained conditions. However, it is the resulting earthquake-induced deformations that are the main concerns to engineers. Evidences from past earthquakes indicate that liquefaction-induced large (in the order of meters) lateral spreads and flow slides have taken place in relatively gentle (no more than a few percent) coastal or river slopes in many regions of the world (Kokusho, 2003). Seismically triggered submarine slides and marine structure failures were also reported/summarized by Scott and Zukerman (1972); Hamada (1992) and Sumer et al (2007). More interestingly, flow slides have occurred not only during but also after earthquake shaking.

Two key factors controlling the response of a liquefiable soil deposit to earthquake excitations are:

- Mechanical conditions
- Flow conditions

Mechanical conditions encompass soil density, stiffness and strength, initial static stress state, and earthquake characteristics (amplitude, predominant periods, etc.) that are mostly responsible for the generation of excess pore pressure during seismic loading. The flow conditions i.e. drainage path, soil permeability and its spatial variation (permeability contrast) within the soil deposit control the redistribution of excess pore pressure during and after the earthquake. Sharp et al. (2003) and Seid-Karbasi and Byrne (2006a) used centrifuge model tests and numerical analyses, respectively, demonstrated that liquefiable soil deposits with lower permeability suffer greater deformations in an earthquake.

Seid-Karbasi and Byrne (2006a) also showed that pore water migration is likely responsible for liquefaction onset commonly observed first at shallower depths of uniform soil layers in past earthquakes and physical model tests.

The majority of the previous liquefaction studies were based on the assumption that no flow occurs during and immediately after earthquake loading and were centered on mechanical conditions. However, this condition may not represent the actual conditions, because both during and after shaking, water migrates from zones with higher hydraulic head (e.g. greater excess pore pressure) towards zones with lower hydraulic head (excess pore pressure). Recent studies including field investigation by Kokusho and Kojima (2002), physical model testing by Kukosho (1999) and Kulasingam et al. (2004), and numerical analysis by Seid-Karbasi and Byrne (2004a) and Seid-Karbasi and Byrne (2007) show that the presence of low permeability sub-layers acting as hydraulic barriers is likely the cause of flow failures of slopes underlain by loose sandy soils. The presence of such a hydraulic barrier layer impedes the upward flow of water resulting in a very loose zone immediately below the barrier leading to significant strength loss and possible post-shaking failure. This mechanism is also referred to as "void redistribution" since it tends to develop a contracting zone in the lower parts of the liquefied sand layer and an expanding zone in the upper parts of it. The severe strength loss due to expansion can lead to flow failures even in very gentle slopes and after shaking has ceased as demonstrated by Seid-Karbasi and Byrne (2007).

This paper presents the results of a dynamic, coupled stress-flow analysis completed for the examination of the response of an LNG marine terminal foundation slope underlain by a clayey layer which overlies a loose to compact sand deposit located in a region of relatively low level of seismicity (PGA < 0.15g).. Artesian groundwater conditions are present at the site since the pervious sand layer is hydraulically connected to the upland areas, and were considered in the analysis. The results of the study demonstrate the impact of a low permeability-layer on the seismic behavior of slopes and earth structures.

SAND LIQUEFACTION AND FLOW CONDITIONS

Earthquake-induced soil liquefaction refers to a sudden loss in shear strength and stiffness due to seismic shaking. The loss arises from a tendency for granular soil to undergo volume change when subjected to cyclic loading. When the volume change tendency is in contraction and the actual volume change is prevented or curtailed by the presence of pore water that cannot escape in time, the pore water pressure will increase and the effective stress will decrease. If the effective stress drops to zero (100% pore water pressure rise), the shear strength and stiffness will also drop to zero and the soil will behave like a heavy liquid.

Although a large number of laboratory investigations on liquefaction resistance of sands have been carried out, most of them dealt with the undrained (constant volume) behavior. Recent laboratory studies, (e.g. Vaid and Eliadorani, 1998; Eliadorani, 2000) demonstrated that a small net flow of water into an element (injection) causing it to expand can result in additional pore pressure generation and further reduction in strength. Chu and Leong (2001) reported that the same phenomenon occurs in loose and dense sand, and called it "pre-failure instability".

Vaid and Eliadorani (1998) examined this phenomenon by injecting or removing small volumes of water from the sample during monotonic triaxial testing as it was being sheared and referred to this as a "partially drained condition" (this test method is also called "strain path" e.g. Chu and Leong 2001). The results of inflow tests on Fraser River sand shown in Fig. 1 in terms of stress path, axial strain vs. time and strain path (with Dr_c= 29%) indicate a potential for triggering liquefaction at constant shear stress ($\sigma'_1 - \sigma'_3 =$ constant). A small amount of expansive volumetric strains imposed by water inflow resulted in an effective stress reduction and flow failure of samples of sand consolidated to an initial stress state corresponding to $R_c = \sigma'_{1c}/\sigma'_{3c} = 2$, as shown in Fig. 1b, where R_c is the effective stress ratio, and σ'_{1c} and σ'_{3c} are the major and minor principle effective stresses, respectively. Chu and Leong (2001) defined this condition as instability that occurs when a soil element subjected to small effective stress perturbation cannot sustain the current stress state and results in runaway deformations as seen in Figs. 1c and 1d, or liquefaction flow. As shown in Fig. 1d, the sample with σ'_{3c} = 100 kPa failed once the volumetric strain (ε_v) reached about 0.2%. In these tests, expansive ε_v was imposed by injection of water into the samples (see Fig. 1a) at a constant rate of $d\varepsilon_v/d\varepsilon_1$ = -0.4, where ε_1 is the axial strain. The samples were stable under the initial stress state. The stress paths during injection indicate a reduction in effective stresses at a constant shear stress. For each sample with each different initial confining stress as shown in Fig. 1d, the large reduction of shear strength/stiffness (i.e. instability) occurred with little change in shear stress and void ratio and at very small ε_1 of the order of 0.5%. Positive pore pressures continued to develop even beyond the phase transformation line. This occurs because the rate of imposed expansive volumetric strain is greater than the dilation potential of the soil skeleton in drained conditions.

Yoshimine et al. (2006), Sento et al. (2004) and Bobei and Lo (2003) reported similar responses for Toyoura sand and silty sand. As a result, soil elements may liquefy due to expansive volumetric strains that cannot be predicted from analyses based on the results of undrained tests.

The stability conditions of a saturated slope under seismic loads depends largely on whether soil liquefaction will be triggered and what level of soil shear strength and stiffness loss would occur, which in turn depends on the relative rate

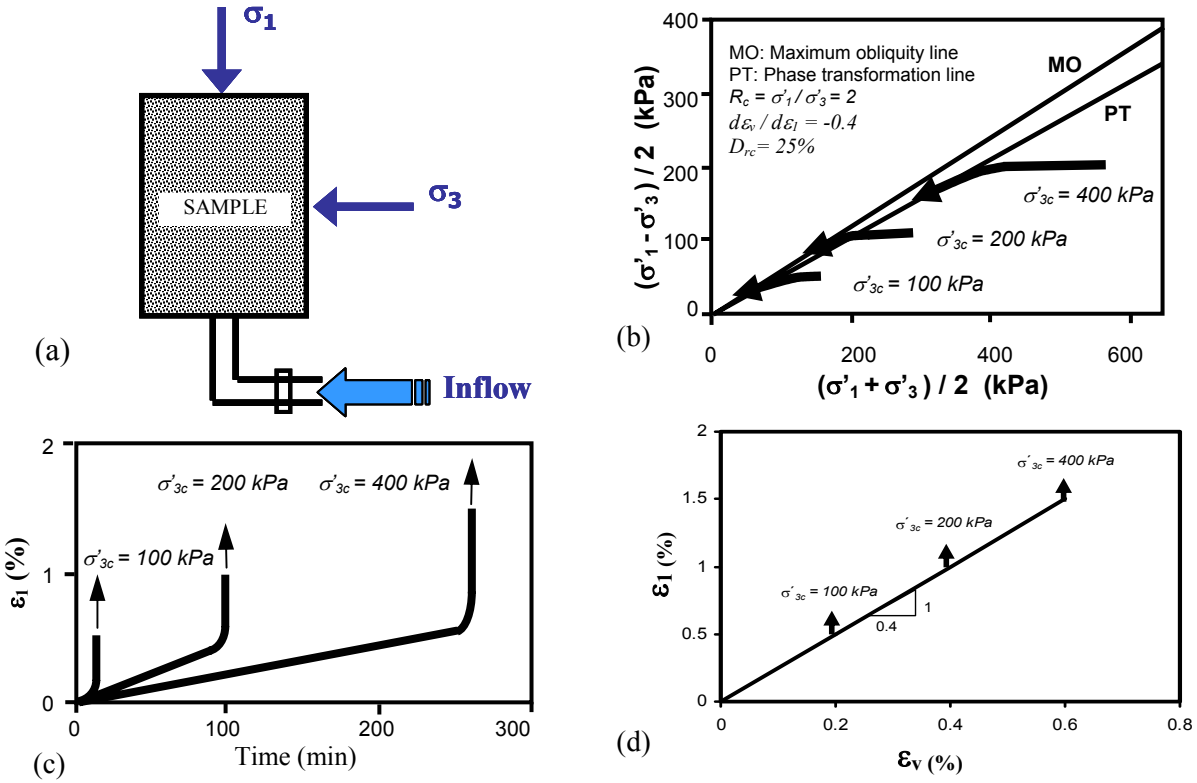

Fig. 1. Partially-drained instability of loose Fraser River sand (data from Vaid and Eliadorani 1998): (a) inflow into triaxial sample (b) stress paths; (c) strain paths and (d) axial strain vs. volumetric strain.

of pore pressure generation due to seismic shaking and pore pressure dissipation due to drainage. The potential for large lateral displacements or flow slides will be greatly increased if a low permeability layer (e.g. a silt or clay layer) within a soil deposit forms a hydraulic barrier and impedes drainage. The excess pore water generated by seismic loading generally drains upwards and may accumulate underneath the hydraulic barrier layer to form a water film if the water inflow to the soil elements immediately below the barrier exceeds the elements' ability to expand (net inflow). This may result in the formation of a thin layer of soil with near-zero shear strength and eventually flow failure (Seid-Karbasi and Byrne, 2007a). Based on the results of a numerical analysis completed on an idealized infinite slope underlain by a low-permeability layer which overlies a liquefiable sand layer, Seid-Karbasi and Byrne (2007b) demonstrated that expansion occurs at the upper parts of the liquefiable soil layer while the lower parts contract regardless of the thickness of the liquefiable layer. Figure 2 shows a typical volumetric strain profile along the normalized depth of the liquefiable soil layer beneath the hydraulic barrier.

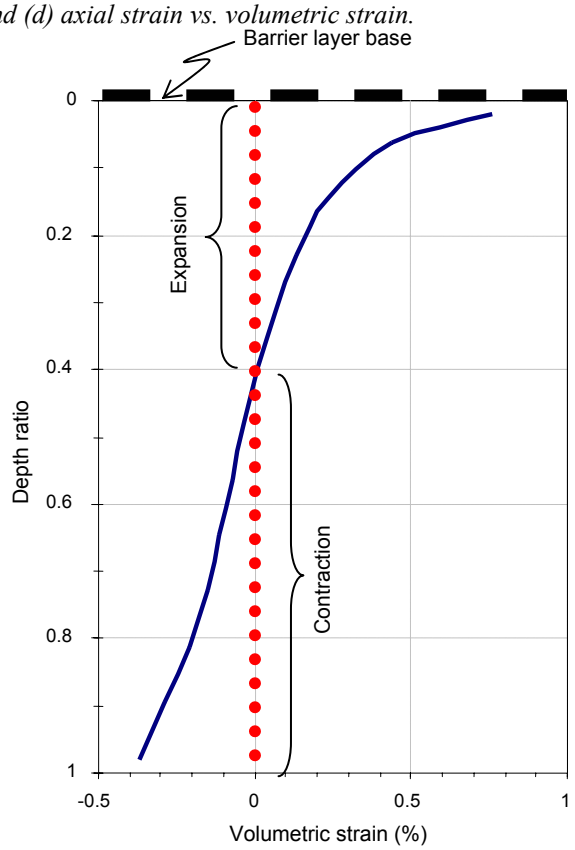

Fig. 2. Typical volumetric strain isochrone beneath the barrier layer with normalized depth for infinite slopes (Seid-Karbasi & Byrne, 2007b).

ANALYSIS PROCEDURE

In order to evaluate the impact of a low permeability layer on the earthquake-induced ground deformations, it is necessary to simulate the generation, redistribution, and dissipation of excess pore pressures during and after earthquake shaking. This approach requires a coupled

dynamic stress-flow analysis. In such an analysis, the volumetric strains of the soil skeleton are controlled by the compressibility of the pore fluid and flow of water through the soil elements. To predict the instability and liquefaction flow, an effective stress-based elastic–plastic constitutive model (*UBCSAND*) was used. The model was calibrated using laboratory and centrifuge test data and is described below.

Constitutive Model for Sands

The *UBCSAND* constitutive model is based on the elasto-plastic stress–strain model proposed by Byrne et al. (1995), and has been further developed by Beaty and Byrne (1998) and Puebla (1999). The model has been successfully used in analyzing the CANLEX liquefaction embankments (Puebla et al., 1997) and predicting the failure of Mochikoshi tailings dam (Seid-Karbasi and Byrne 2004b). It has also been used to examine partial saturation conditions on liquefiable soil's response (Seid-Karbasi and Byrne, 2006) and dynamic centrifuge test data (e.g. Byrne et al., 2004 and Seid-Karbasi et al., 2005). It is an incremental elasto-plastic model in which the yield loci are lines of constant stress ratio ($\eta = \tau / \sigma'$). Plastic strain increments occur whenever the stress ratio increases. The flow rule relating the plastic shear strain increment direction to the volumetric strain increment direction is non-associated, and leads to a plastic potential defined in terms of the dilation angle. Plastic contraction occurs when stress ratios are below the constant volume friction angle and dilation occurs otherwise, as shown in Fig. 3.

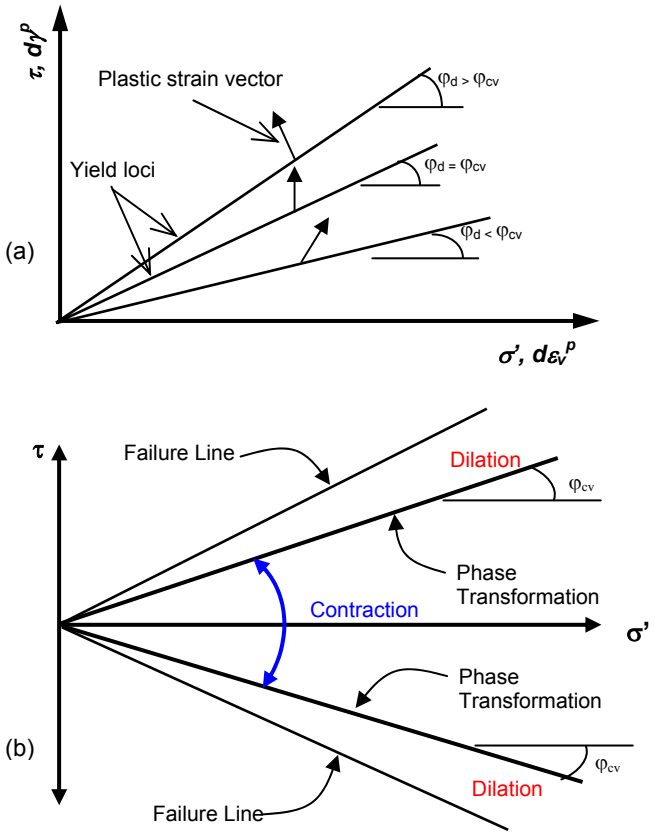

Fig. 3. (a) moving yield loci and plastic strain increment vectors, (b) dilation and contraction regions.

The elastic component of the response is assumed to be isotropic and defined by a shear modulus, G^e, and a bulk modulus, B^e, as shown in Eq. 1 and Eq. 2,

$$G^e = K^e_G . P_a \left(\frac{\sigma'}{P_a} \right)^{n_e} \quad (1)$$

$$B^e = \alpha . G^e \quad (2)$$

where K^e_G is the shear modulus coefficient, P_a represents the atmospheric pressure, $\sigma' = (\sigma'_x + \sigma'_y) / 2$, n_e is an empirical parameter depending on the soils (commonly 0.5), α depends on soil's elastic Poisson's ratio (varies from 0 to 0.2 as suggested by Hardin and Drnevich, 1972) and ranges from 2/3 to 4/3. The plastic shear strain increment $d\gamma^P$ and plastic shear modulus are related to stress ratio, $d\eta$ ($\eta = \tau / \sigma'$) as expressed by Eq. 3:

$$d\gamma^p = \left(\frac{d\eta}{\left(\frac{G^p}{\sigma'} \right)} \right) \quad (3a)$$

$$G^p = G^p_i \left(1 - \frac{\eta}{\eta_f} R_f \right)^2 \quad (3b)$$

where G^P is the plastic shear modulus defined by a hyperbolic function as Eq. 3b, G^P_i is the plastic shear modulus at very low stress ratio level (η near 0), $\eta_f = \sin\varphi_f$ is the stress ratio at failure, where φ_f is the peak friction angle, and R_f is the failure ratio. The associated increment of plastic volumetric strain, $d\varepsilon_v^P$, is related to the increment of plastic shear strain, $d\gamma^P$, through the flow rule as shown in Eq. 4:

$$d\varepsilon_v^P = d\gamma^P . (\sin\varphi_{cv} - \eta) \quad (4)$$

where φ_{cv} is the friction angle at constant volume (phase transformation). It may be seen from Eq. 4 that at low stress ratios ($\eta = \tau / \sigma' = \sin\varphi_d$) significant shear-induced plastic compaction is predicted to occur, while no compaction would occur at stress ratios corresponding to φ_{cv}. For stress ratios greater than φ_{cv}, shear-induced plastic expansion or dilation is predicted. More detailed discussions about the UBCSAND constitutive model were presented previously in Byrne et al. (2004) and Puebla et al. (1997).

The constitutive behavior of sand is controlled by the skeleton. The pore fluid (e.g. water) within the soil mass acts as a volumetric constraint on the skeleton if drainage is fully or partially curtailed. This model has been

incorporated into the commercially available computer code FLAC (Itasca, 2005).

The key elastic and plastic parameters can be expressed in terms of relative density, *Dr,* or normalized Standard Penetration Test values, $(N_1)_{60}$. Initial estimates of these parameters were developed from published data and model calibrations. The responses of sand elements under monotonic and cyclic loading were then predicted and the results compared with the laboratory data. The predictions from the model were matched with the observed responses for sandy soils with a range of relative density or N values. The model was calibrated to reproduce the NCEER 97 chart, which, in turn, is based on field data during past earthquakes and is expressed in terms of normalized Standard Penetration Test, $(N1)_{60}$. The model properties to obtain such agreement are therefore expressed in terms of $(N_1)_{60}$ values.

Model Simulation of Laboratory Element Tests

The UBCSAND model was applied to simulate cyclic simple shear tests under undrained condition. Figure 4 shows model predictions along with test results on Fraser River sand. The sand tested had an initial vertical consolidation stress σ'_v = 100 kPa and relative density *Dr* = 40%.

The results of the model prediction, expressed in terms of stress-strain and excess pore pressure ratio, *Ru,* and stress path, compared reasonably well with the laboratory data as shown in Fig.4. It should be noted that as unloading is considered elastic, the excess pore pressure is constant while unloading takes place during cyclic shearing. A comparison of model prediction with tests results in terms of required number of cycles to trigger liquefaction for different cyclic stress ratios, *CSR* is shown in Fig. 3c and reasonable agreement is observed. The predicted apparent step-wise increase in the excess pore pressure with the number of cycles is numerically induced. This is because the cycle count is updated at every half cycle and the pore pressure itself is computed at every step.

The model was also used to study the effects of both the undrained and the partially drained conditions and the model predictions were compared with the observations during triaxial monotonic tests. The partial drainage tests involved injecting water into the sample to expand its volume as it was sheared. The injection causes a drastic reduction in soil strength. The same amount of volumetric expansion was applied in the numerical model and the results shown in Fig. 5 (solid line for model prediction) are in good agreement with the measured data. The above simulations illustrate that the model can appropriately simulate the pore pressure and stress-strain response under undrained loading, and can also account for the effect of volumetric expansion caused by inflow of water into an element.

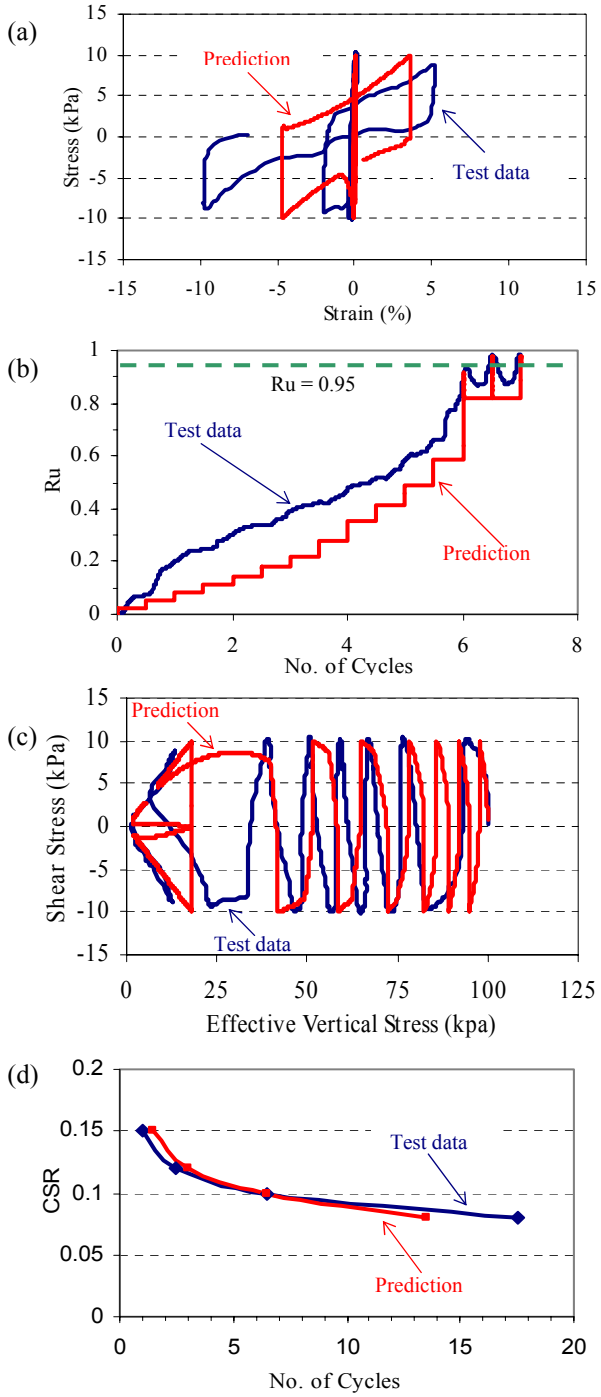

Fig. 4. Comparison of predicted and measured response for Fraser River Sand, D_r = 40% & σ'_v = 100 kPa (a) stress-strain, CSR = 0.1, (b) R_u vs. No. of cycles (liquefaction: $R_u \geq 0.95$), (c) CSR vs. No. of cycles for liquefaction (tests data from Sriskandakumar, 2004).

PROJECT DESCRIPTION AND SITE CONDITIONS

The development of an LNG import facility in Bish Cove, Kitimat, BC, Canada is currently being considered. The project site is located about 12 km south of Kitimat city center on the west bank of Kitimat Arm (Douglas Channel). The offshore portion of the project includes the main LNG

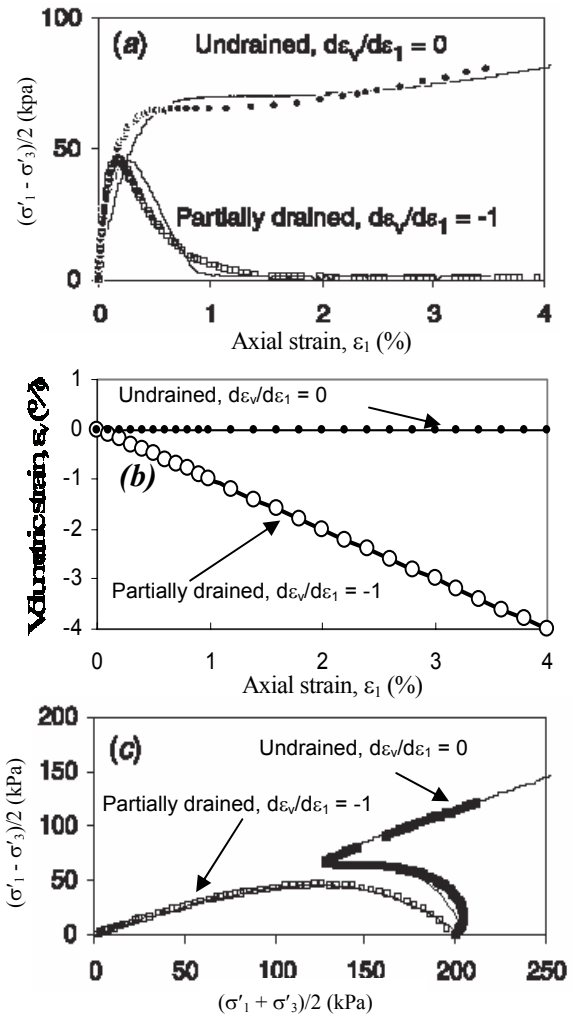

Fig. 5. Soil element response in undrained and partially drained (inflow) triaxial tests for FR River sand, (a) stress-strain, (b) volumetric strain, and (c) stress paths (modified from Atigh and Byrne 2004).

tanker jetty and a construction berth to be built along the northern shoreline of Bish Cove. The major components of the LNG tanker jetty include the LNG unloading platform, 4 berthing dolphins, and 6 mooring dolphins connected from one end to the other end by catwalks/gangways. Large diameter (914 mm to 1,067 mm) steel pipe piles installed into bedrock will provide foundation support to the LNG jetty structures. The seabed elevation along the alignment of the jetty will be about -20 m (Geodetic Datum), which is about 17 m below the mean sea level at the site. The seabed surface in the inter-tidal zone (between the high high water and low low water) slopes gently at 4 to 15% down to the south (towards the ocean), and the sub-tidal zone slopes gently to moderately (from less than 20% to more than 40% locally). The bedrock surface slopes to the south, and undulates significantly with elevations varying from about 0 m or higher (outcropping) locally to about -55 m near the eastern mooring dolphin.

The site is located in a zone of moderate seismicity, and the peak horizontal firm-ground acceleration (PGA) for Class C ground conditions is 0.13 g based on the 4th Generation Seismic Hazard Maps developed by the Geological Survey of Canada (GSC) as input to the 2005 National Building Code of Canada (NBCC). Due to the presence of bedrock corresponding to Class A ground conditions, the applicable site-specific peak firm ground acceleration value is decreased from 0.13 g to 0.09 g for design purposes for ground motions with a return period of 1 in 2,475 years.

Historical evidence shows that a large number of submarine landslides have occurred along the west coast of British Columbia and Alaska (Bornhold et al, 2001). The 1964 Good Friday earthquake triggered several submarine landslides in Valdez and Sayward Ports, Alaska. Other slides have been triggered by construction activities undertaken at low tides (i.e. Moon Bay, Kitimat in 1975). Regardless of the triggering mechanism, submarine slope failures are a direct threat to structures such as offshore jetties, pipelines, cables, and to the environment.

Subsurface Soil and Groundwater Conditions

Geotechnical and geophysical investigations were carried out by Golder Associates Ltd. (Golder) to obtain information on subsurface soil and bedrock conditions at the jetty site. Based on results of these investigations, the site is inferred to be underlain by a layer of soft to very soft clayey soils extending from seabed surface to depths of about 6 m to 13 m. The clayey soil overlies a deposit of very loose to compact sand and silty sand extending to depths of some 10 m to 30+ m below seabed. The sand deposit is underlain by strong granitic bedrock.

Steep mountain slopes are present to the north and west of the project site, and site groundwater conditions are affected by the regional groundwater regime, which is, in turn, affected by the seasonal variation of weather conditions. The daily sea level fluctuations (tides) also affect the local groundwater regime in the inter-tidal and sub-tidal zones. Due to the presence of sloping ground conditions and a low-permeability clayey layer overlying the high-permeability sandy layer, artesian water conditions exist within the sand stratum and in the offshore areas during wet months of a given year and/or at low tides.

Artesian groundwater conditions were observed during an offshore drilling investigation carried out at the project site (by others) in February, 1997. Sustained and high volume (40 to 50 gpm) of artesian water flow was observed during a 2007 onshore investigation carried out by Golder at a site with a similar geological setting (about 6 to 8 km south of the subject site and on the western shore of Kitimat Arm).

Artesian water conditions were not visually detected during the 2006 Golder offshore investigation carried out at the project site. However, the presence of artesian conditions

can be inferred from the pore water pressures recorded in a CPT test as shown in Fig. 6. After penetrating through the clay/silt deposit, the CPT was advanced into the relatively clean sand encountered at a depth of about 13 m. The pore pressures recorded in the clean sand represent the 'steady-state' water pressures near the tip of the cone. As shown in the pore pressure plot (U2 and Uh between 13 and 15.4 m depths) included in Fig. 6, the straight line represents the pore water pressure calculated based on the water depth (tidal variation has been considered), and the irregular line represents the actual pore pressure recorded during CPT testing. The gap between these two lines indicates that excess water pressure in the sand stratum over and above the hydrostatic pressure. Fig. 7 shows the values of artesian pore pressure estimated based on the CPT results. For clarity of presentation, Fig. 7 (a) shows a reproduction of the section of the CPT log, the segment of the pore water plot between 13.4 m and 15.4 m. Fig. 7 (b) shows the estimated head of the artesian pressure, which is estimated to be about 3.3 m.

Previous Landslides along the Coast of Pacific Northwest

A large number of coastal and submarine landslides have

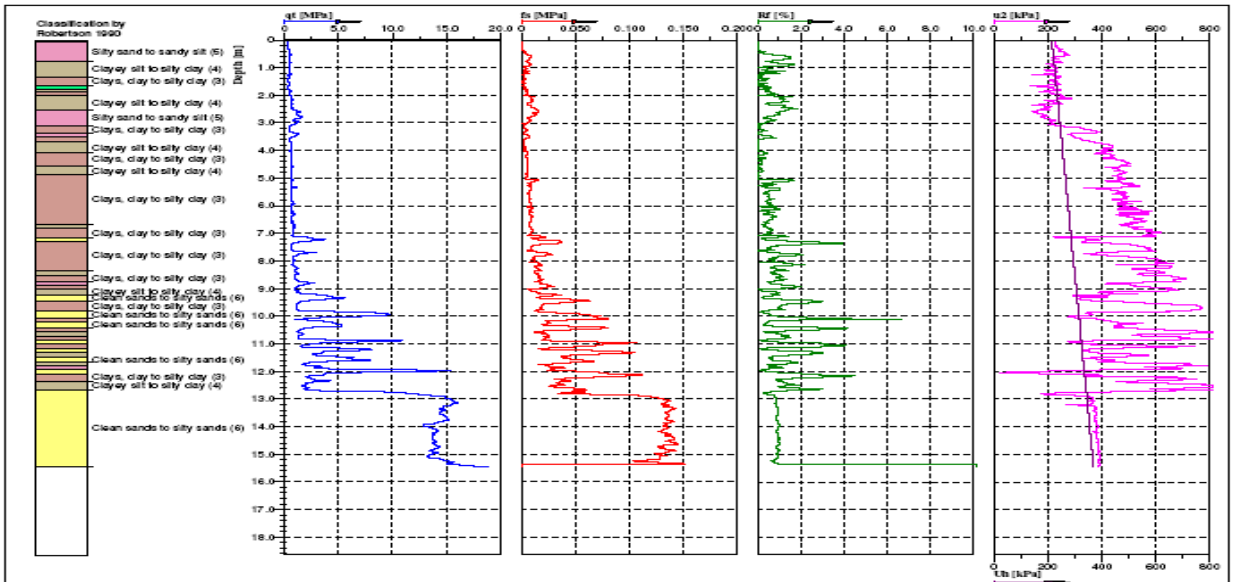

Fig. 6. Records of a static cone penetration test (CPT06-1) completed at the project site in 2006.

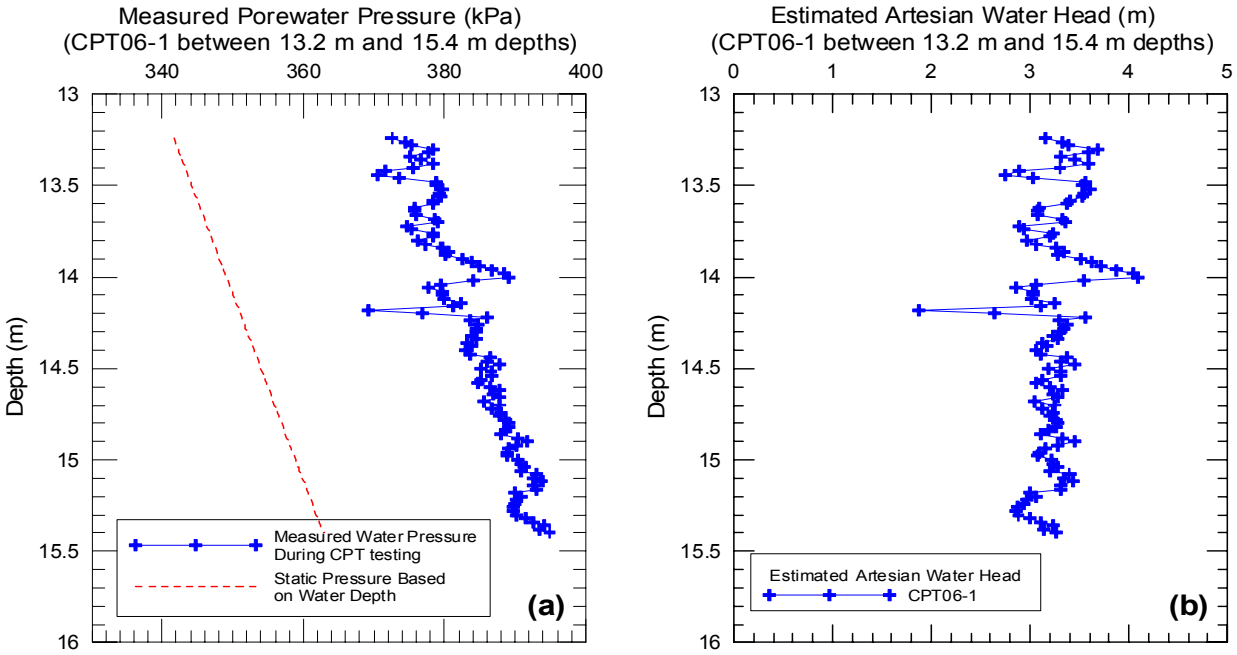

Fig. 7. Measured pore water pressure and estimated artesian water head at CPT06-1 location.

occurred along the west coast of British Columbia and Alaska. A map showing the locations of recorded major historical landslides is reproduced in Fig. 8. A series of submarine landslides have occurred in Kitimat Arm over the period extending from 1952 to 1975 (Bornhold et al, 2001). The most recent Moon Bay (6 to 8 km south of the subject site) submarine slide occurred at 10:05 a.m. on April 27, 1975 shortly after low tide and coincided with the construction of an offshore jetty. It is reported that the 1964 and 1994 Skagway submarine slides also occurred at extreme low tides. The 1964 "Good Friday" earthquake is reported to have triggered several submarine landslides. The historical evidence indicates that coastal submarine slope failures can be triggered by construction activities under low tides or by earthquake loading when the delicate equilibrium attained by long-term ambient conditions is disrupted.

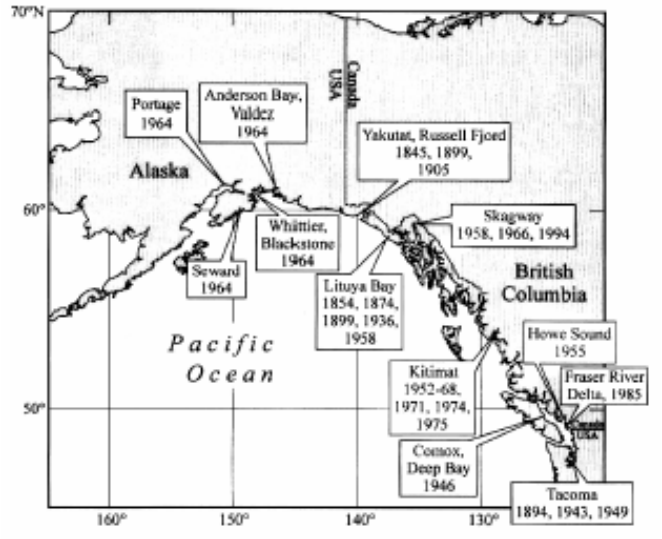

Fig. 8. Locations of major historical coastal and underwater landslides (Bornhold et al, 2001).

The cross-section of the near-shore slope used in the 2-dimensional (2D) FLAC analysis is shown in Fig. 9. The 2D FLAC model extended about 275 m landward from the centerline of the mooring dolphin structure and about 325 m seaward from that. The average ground surface inclination is about 20% in the sub-tidal zone, about 4 to 6% in the inter-tidal zone and about 40% in the onshore area above the inter-tidal zone.

UBCSAND model was used to represent the constitutive behavior of the sandy soils, and Mohr-Coulomb model was used to represent the clayey soils. The nonlinearity and energy dissipation mechanism of the clay material during dynamic loading was modeled by UBCHYST model that accounts for the hysteretic damping in fine-grained soils (Byrne, 2006). Based on results of the field investigation, the loose to compact sand layer was assigned a standard penetration resistance $(N_1)_{60}$ value of 10 blows/0.3 m, and the surficial clay layer was assigned an undrained shear strength value of 20 kPa in the zone below mean sea level, and 30 kPa in zones further upland,

The hydraulic conductivity of the sandy soil was estimated to be 1.0e-4 m/s based on grain size distribution of samples collected from the site during the geotechnical investigation. The sand permeability in vertical direction was assumed to be 1/2 of that in the horizontal direction. The hydraulic conductivity of the clayey soil was estimated to be 100 times lower than that of the underlying sandy soil.

The artesian conditions equivalent to about 3.3 m of excess water head within the sandy soil layer were established by modelling the groundwater seepage flow using the FLAC model. It was assumed that the groundwater level within the onshore portion of the slope is about 3.3 m higher than the mean sea level. The groundwater model was solved to reach a "steady state" of flow and pressure distribution (or gradient) prior to the application of seismic shaking.

NUMERICAL MODELING, PARAMETERS AND

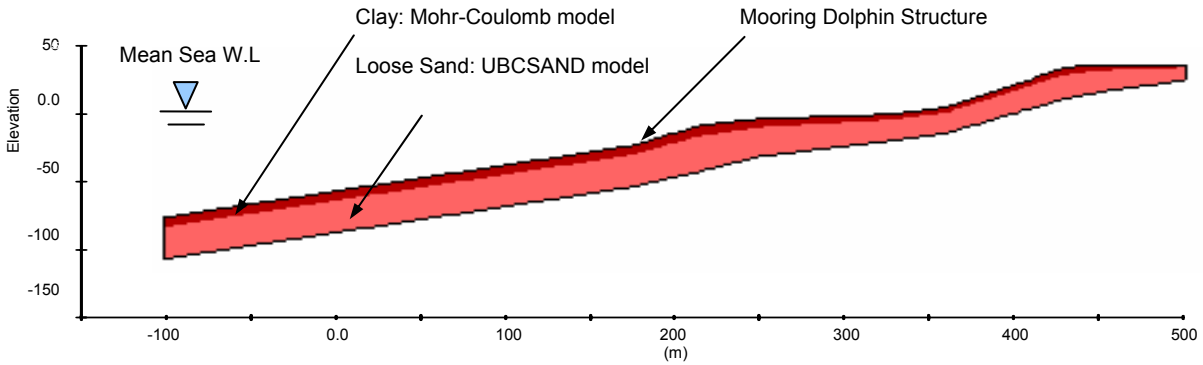

Fig. 9. FLAC model of soil foundation with different material types.

GROUND MOTIONS

The earthquake acceleration time-histories were spectrally matched to the GSC Site Class A bedrock response spectrum that corresponds to a return period of 1 in 2475 years. The peak firm-ground acceleration that corresponds to Class A rock conditions is about 0.13 g. The input motions developed from 1-D analysis employing ProShake (EduPro Civil Systems, 2001) computed at the top of the bedrock (as within motions) were applied at the base of the FLAC model. One of the representative base motion input time-histories used in the FLAC analysis is shown in Fig. 9. As shown in the figure, the total duration of earthquake shaking is about 20 seconds with the duration of strong shaking being less than 6 to 7 seconds, and the PGA value of the input motion is about 0.09 g.

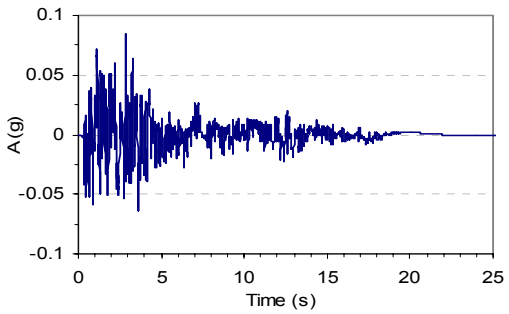

Fig. 10. Base acceleration time history.

Results and Discussion

The computed ground surface horizontal displacements are about 250 mm in the vicinity of the mooring dolphin structure at the end of earthquake shaking, and the deformed grid in this area is shown in Fig. 11. As shown in the figure, large deformation (strain) occurred within the sand layer immediately below the clay stratum. The horizontal displacement distribution along the depth of soils at the dolphin location is shown in Fig. 12, which demonstrates more clearly the highly concentrated strains occurred at the sand-clay interface.

Fig. 13 shows the computed time history of horizontal displacement at the dolphin location together with the base (bedrock) motion velocity time history. As shown in the figure, the displacement increases at a near constant rate after the earthquake excitations have completely terminated. In other words, the slope keeps moving even after seismic shaking has ceased. This indicates that the excess pore water pressures generated due to earthquake shaking in combination with the artesian water conditions have a high potential to destabilize the slope and induce large slope movements at the site.

The predicted seismic response (i.e. the concentration of strain and deformation at the clay-sand interface and continued deformation after shaking cease reflects the characteristic feature of a slope whose behaviour is affected

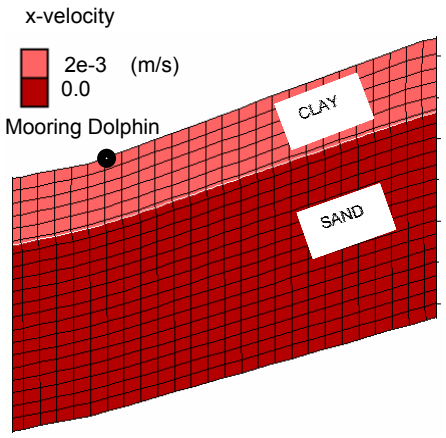

Fig. 11. Distribution of x-velocity within the foundation in the vicinity of mooring dolphin at 50 s.

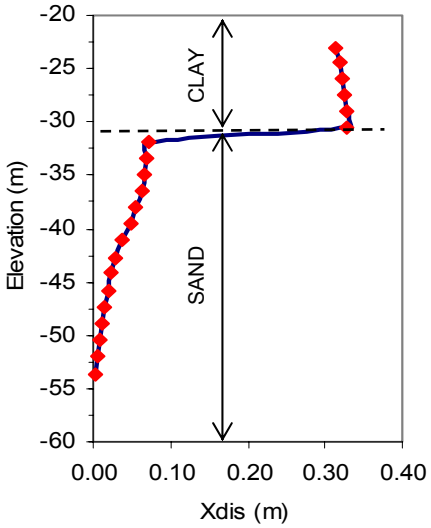

Fig.12. Lateral displacement profile at mooring dolphin location.

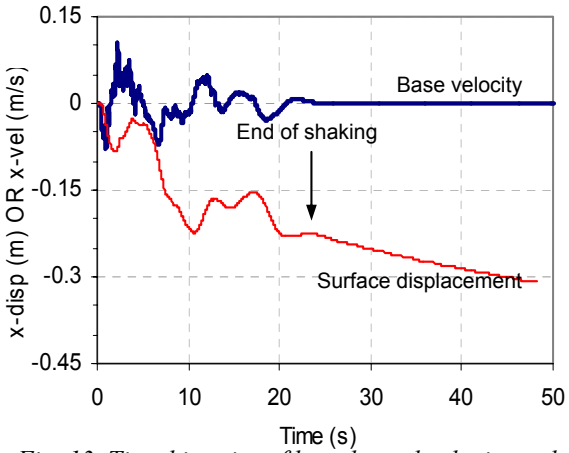

Fig. 13. Time histories of base lateral velocity and surface lateral displacement.

by the presence of a hydraulic barrier as reported by previous studies using centrifuge testing and numerical modeling (e.g. Kulasingam et al. 2004 and Seid-Karbasi and Byrne, 2007). Fig. 14 shows the deformation pattern observed in a centrifuge model of a slope with silt layer inclusion (Kulasingam et al., 2004) which indicates a localized deformation concentration immediately beneath the hydraulic barrier layer. Also, the delay and increasing effects of barrier layer on displacements can be seen from Fig. 15 that shows the predicted time history of surface lateral displacement for an infinite 1°-slope with and without low permeability layer (Seid-Karbasi and Byrne 2007).

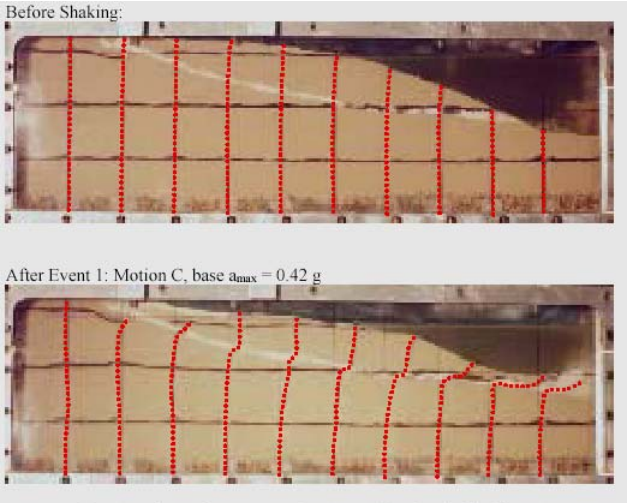

Fig. 14. Deformation pattern with localization observed in centrifuge model of a slope with barrier layer (Kulasingam et al. 2004)

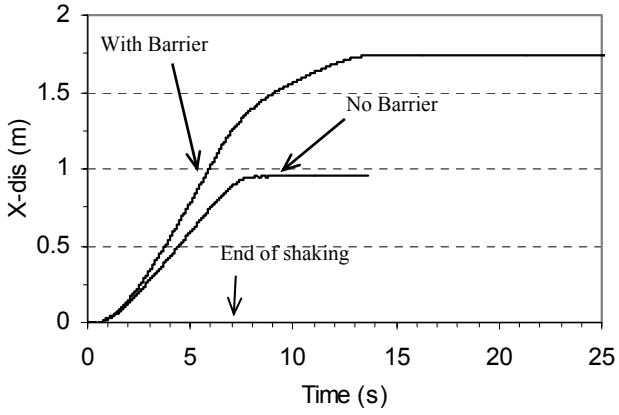

Fig. 15. Time history of surface lateral displacement for a 10 m-liquefiable slope with and without barrier layer indicating post shaking deformation due to hydraulic barrier effects (Seid-Karbasi and Byrne, 2007).

A number of additional cases were also analyzed for the Bish Cove slope to study the impact of the variations of the artesian water conditions on the seismic stability of the slope and to provide input to the design of soil improvement measures. The results of the analyses show that the stability conditions of the slope can be significantly enhanced such that large earthquake-induced slope displacements can be prevented if appropriately designed soil improvement measures are implemented.

CONCLUSIONS

The seismic stability of a gentle near-shore slope underlain by an upper clay layer overlying loose to compact sands was studied using an effective stress-based, coupled mechanical-flow, dynamic analysis. The following presents a summary of the conclusions of the study.

1) The presence of a low-permeability sub-layer (hydraulic barrier) is one of the primary causes of artesian groundwater conditions. The hydraulic barrier also blocks or retards the upward flow arising from excess pore pressures generated by earthquake shaking and causes the pore pressures to remain high for some time after strong shaking. The effect of artesian and earthquake-generated pore pressures are additive and both arise from the permeability contrast between the upper clay unit and the underlying sand.

2) Under seismic loading conditions, large lateral deformations (or strains) are likely to occur within a thin layer of liquefied sand located immediately underneath the clay layer. This thin layer is likely to suffer significantly more strength and stiffness loss than the soils further below due to the presence of the hydraulic barrier. A failure plane (localization) may develop within this thin and weakened layer.

3) Even for a gentle slope located within a region with low to moderate design earthquake intensity, large slope displacements or even a post-shaking flow slide may still occur due to the unfavourable subsurface soil and groundwater conditions.

4) Based on review of the information from a number of historical coastal and submarine landslides and previous physical and numerical investigations together with the results of this study, it is inferred that the presence of a relatively continuous low permeability silt or clay layer that form a hydraulic barrier is a major cause of catastrophic failures of gentle slopes.

5) The stability conditions of the slope at Bish Cove were further evaluated assuming that measures will be implemented to improve the soil and reduce the artesian pore water pressure. The results of the evaluation indicate that appropriately designed soil improvement

measures can strengthen the slope sufficiently and prevent the occurrence of large slope displacements.

6) As soil permeability is a key issue in seismic performance of earth structures, it is essential to employ appropriate investigation procedures to detect and characterize different materials and permeability contrasts within man-made and/or natural foundations

ACKNOWLEDGEMENTS

The authors would like to thank Mr. Al Tsuji and Kitimat LNG Inc. for giving permission to publish the results of the field investigation and engineering analyses performed by Golder Associates Ltd. in this paper.

REFERENCES

Atigh, E. and Byrne, P. M. 2004. "Liquefaction Flow of Submarine Slopes under Partially Undrained Conditions: An Effective Stress Approach", Can. Geotechnical J., V. 41, pp. 154-165.

Beaty, M. H. and Byrne, P. M. 1988. "An Effective Stress Model for Predicting Liquefaction Behavior of Sand", *Proc., Conf., Geotech.Eq.Engg. & Soil Dyn.III*, ASCE GSP No. 75, V1, pp. 766-777.

Bobei, D.C., and Lo, S-C. 2003. "Strain Path Influence on the Behavior of Sand with Fines", *Proceedings, 12th Panamerican Conference on Soil Mechanics and Geotechnical Engineering, Soil and Rock America 2003*, MIT, Cambridge, Massachusetts, pp. 583-588.

Bornhold, B.D., Thompson, R., Rabinovich, A., Kulikov, E. and Fine, I. 2001. "Risks of Landslides-Generated Tsunamis for the Coast of British Columbia and Alaska", *Proc. 54th Canadian Geotechnical Conference*. pp. 1450-1454.

Byrne, P.M., Roy, D., Campanella, R.G., and Hughes, J. 1995. "Predicting Liquefaction Response of Granular Soils from Pressuremeter Tests", *ASCE National Convention, ASCE, GSP 56,* pp. 122-135.

Byrne, P.M., Park, S., Beaty, M., Sharp, M., Gonzalez, L. and Abdoun, T. 2004. "Numerical Modeling of Liquefaction and Comparison with Centrifuge Tests", Can. Geotech. J., V. 41, pp. 193-211.

EduPro Civil Systems, 2001. "Proshake, Ground Response Analysis", Version 1.1 , *User's Manual,* EduPro Civil Systems Inc. Redmond, Washington.

Eliadorani, A. 2000. "The Response of Sands under Partially Drained States with emphasis on Liquefaction", *PhD.Thesis, Civil Engg.* Dept., the University of British Columbia, Vancouver, B.C.

Hardin, B. and Drnevich, V. "Shear Modulus and Damping in Soils: Deign Equations and Curves", J., Soil Mech., & Found. Engg., ASCE, V. 98, pp. 667-692, 1972.

ITASCA, 2005. "Fast Lagrangian Analysis of Continua (FLAC)", Version 5, *User's Guide.* Itasca Consulting Group, Inc.

Kokusho, T. 1999. "Water Film in Liquefied Sand and its effect on Lateral Spread", Journal of. Geotechnical and Geo-Environmental Engineering, ASCE, V. 125, pp. 817–826.

Kokusho, T. 2003. 'Current State of Research on Flow Failure Considering Void Redistribution in Liquefied Deposits", J., Soil Dynamics and Earthquake Engineering, V. 23, pp. 585–603, 2003.

Kulasingam, R., Malvick E. J., Boulanger, R. W. and Kutter, B.L. 2004. "Strength Loss and Localization at Silt Interlayers in Slopes of Liquefied Sand", J.,Geotech., & Geoenviron.Engg., ASCE, V. 130, pp. 1192-1202, 2004.

Puebla, H. 1999. "A Constitutive Model for Sand Analysis of the CANLEX Embankment", *PhD. Thesis, Civil Engg. Dept.*, Un., British Columbia, Vancouver, B.C.

Puebla, H., Byrne, P. M., and Phillips, R. 1997. "Analysis of CANLEX Liquefaction Embankment: Prototype and Centrifuge models", Canadian Geotechnical J., 34, pp. 641-654.

Seid-Karbasi, M., Byrne, P. M. 2004a. "Liquefaction, Lateral Spreading and Flow Slides", *Proc. 57th Canadian Geotechnical. Conf.*, p. G13.529.

Seid-Karbasi, M. and Byrne, P. M. 2004b. "Embankment Dams and Earthquakes", Hydropower and Dams J., V.11(2), pp. 96-102.

Seid-Karbasi, M., Byrne, P. M., Naesgaard, E., Park, S., Wijewickreme, D., and Phillips, R. 2005. "Response of Sloping Ground with Liquefiable Materials during Earthquake: A Class A Prediction", *Proc., 11th Int. Conf., Int. Ass., Computer Methods & Advances in Geomechanics, IACMAG,* Turin, Italy, V. 3, pp. 313-320.

Seid-Karbasi, M., and Byrne, P. M. 2006a. "Significance of Permeability in Liquefiable Ground Response", *Proc. 59th Canadian Geotechnical. Conf.*, pp. 580-587.

Seid-Karbasi, M., and Byrne, P. M. 2006b. "Effects of Partial Saturation on Liquefiable Ground Response", *Proc., ASCE 2006 Geo-Congress, Geotechnical Engineering in Information Tech. Age*, Atlanta, Gorgia., Paper # 11803.

Seid-Karbasi, M., and Byrne, P. M. 2007a. "Seismic Liquefaction, Lateral Spreading and Flow Slides: A Numerical Investigation into Void Redistribution", *Canadian Geotechnical J.* V. 44, pp. 873-890.

Seid-Karbasi M., and Byrne, P. 2007b. "Characteristic Behavior of Liquefiable Grounds with Low Permeability Sub-Layers", *Proceedings of the 4th Int. Conference on Earthquake Geotechnical Engineering,* Thessaloniki, Greece, Paper # 1173.

Sento, N., Kazama, M., Uzuoka, R., Ohmur, H., and Ishimaru, M. 2004. "Possibility of Post Liquefaction Flow Failure due to Seepage", *Journal of Geotechnical and Geoenvironmental Engineering, ASCE*, V. 130, pp. 707-716.

Sumer, M., Ansal, A., Cetin, O., Damgaard, J. Gunbak, R. Ottesen Hansen, N., Sawicki, A., Synolakis, C., Cevdet Yalciner, A., Yuksel, Y. and Zen, K. 2007. "Earthquake-Induced Liquefaction around Marine Structures", *J.*, Waterway, Port,Coastal. and Ocean. Engg., ASCE, V. 133 (1), pp. 55-82

Vaid, Y.P., and Eliadorani, A. 1998. Instability and Liquefaction of Granular Soils under Undrained and Partially Drained States", Canadian Geotechnical J., V. 35, pp. 1053–1062.

Yoshimine, M., Nishizaki, H., Amano, K., Hosono, Y. 2006. "Flow Deformation of Liquefied Sand under Constant Shear Load and its Application to Analysis of Flow Slide of Infinite Slope", *Soil Dynamics and Earthquake Engineering Journal,* V. 26, pp. 253-264.

Youd, T. L., Idriss, I. M., Andrus, R., Arango, I., Castro, G., Christian, J., Dobry, J., Finn, L., Harder Jr., L., Hynes, H. M., Ishihara, K., Koester, J., Liao, S. S., Marcuson III, W. F., Martin, G., Mitchell, J. K., Moriwaki, Y., Power, M. S., Robertson, P. K., Seed, R. B., and Stokoe II, K. H. 2001. Liquefaction Resistance of Soils: Summary Report from the 1996 NCEER and 1998 NCEER/NSF Workshops on Evaluation of Liquefaction Resistance of Soils, *J., Geotech. and Geoenviron. Engg., ASCE*, V. 127, pp. 817-833.